^{3}He spin exchange cells for magnetic resonance imaging

R. E. Jacob, S. W. Morgan,[a] and B. Saam[b]

Department of Physics, University of Utah, 115 South 1400 East, Salt Lake City, Utah 84112-0830

(Received 11 February 2002; accepted for publication 23 April 2002)

We present a protocol for the consistent fabrication of glass cells to provide hyperpolarized (HP) ^{3}He for pulmonary magnetic resonance imaging. The method for producing HP ^{3}He is spin-exchange optical pumping. The valved cells must hold of order 1 atm·L of gas at up to 15 atm pressure. Because characteristic spin-exchange times are several hours, the longitudinal nuclear relaxation time T_1 for ^{3}He must be several tens of hours and robust with respect to repeated refilling and repolarization. Collisions with the cell wall are a significant and often dominant cause of relaxation. Consistent control of wall relaxation through cell fabrication procedures has historically proven difficult. With the help of the discovery of an important mechanism for wall relaxation that involves magnetic surface sites in the glass, and with the further confirmation of the importance of Rb metal to long wall-relaxation times, we have developed a successful protocol for fabrication of ^{3}He spin exchange cells from inexpensive and easily worked borosilicate (Pyrex) glass. The cells are prepared under vacuum using a high-vacuum oil-free turbomolecular pumping station, and they are sealed off under vacuum after $\geqslant$100 mg of distilled Rb metal is driven in. Filling of cells with the requisite ^{3}He–N_2 mixture is done on an entirely separate gas-handling system. Our cells can be refilled and the gas repolarized indefinitely with no significant change in their wall properties. Relaxation data are presented for about 30 cells; the majority of these reach a "40/40" benchmark: $T_1 > 40$ h, and ^{3}He polarizations reach or exceed 40%. Typical polarization times range from 12 to 20 h; 20% polarization can be achieved in 3–5 h. © *2002 American Institute of Physics.*
[DOI: 10.1063/1.1487438]

I. INTRODUCTION

The past decade has witnessed vigorous progress in the study of hyperpolarized (HP) noble gases and their application to a broad range of problems in physics, chemistry, and biomedicine. Advances are coming in areas as varied as neutron polarizers,[1] measurements of fundamental symmetries,[2] nuclear magnetic resonance (NMR) at surfaces,[3,4] and magnetic resonance imaging of the lung air space.[5,6] In HP gases, enormous nonequilibrium nuclear spin polarizations (of order 0.1) can be attained at room temperature in ordinary magnetic fields *via* optical pumping techniques,[7,8] greatly enhancing the NMR sensitivity of these nuclei. We are concerned here with spin-exchange optical pumping (SEOP)[7] of ^{3}He gas for application to pulmonary magnetic resonance imaging (MRI). The advent of relatively inexpensive high-power diode-laser arrays has paved the way in particular for MRI and other applications requiring large quantities (of order 1 atm·L) of polarized gas, since the quantity is essentially limited by the available laser power.

HP ^{3}He is produced (and often stored) inside a glass spin-exchange cell containing ^{3}He at several or more atmospheres, 50–100 mbar N_2 (a fluorescence-quenching gas necessary for efficient optical pumping[9]), and a macroscopic amount of alkali metal (typically Rb). The cell is heated to 175–220 °C to obtain the optimal Rb vapor density. The laser light, circularly polarized at a frequency corresponding to the D_1 atomic transition in Rb (795 nm) and colinear with a small magnetic field (of order 10 G) is trained on the cell, thus polarizing the valence electron of the Rb atoms. The polarization is thence collisionally transferred to the ^{3}He nuclei.

In this article we present a protocol for the consistent fabrication of spin-exchange cells which will provide liter quantities of highly polarized ^{3}He for pulmonary MRI. These cells must (1) hold a quantity of gas comparable to an average adult's tidal volume ($\approx$0.5 atm·L), (2) be transparent to 795 nm laser light, (3) withstand pressures of up to 15 atm at 200 °C (making efficient use of the spectrally broad diode-laser array by suitably broadening the Rb absorption line[10]), and (4) be valved and refillable for repeated use without altering important cell characteristics (mainly the longitudinal nuclear relaxation rate at the cell surface).

II. WALL RELAXATION

Controlling longitudinal nuclear spin relaxation is critical to optimizing both the polarization and the useful storage time of the gas for applications. In MRI, for example, polarization is directly related to image quality for a given amount of ^{3}He, and the gas often needs to be transported some distance to the MRI scanner without significant polarization loss.

The noble-gas polarization transient $P_N(t)$ during optical pumping is given by

[a]Current address: Biophysics Research Institute, Medical College of Wisconsin, 8701 Watertown Plank Rd., Milwaukee, WI 53226.

[b]Author to whom correspondence should be addressed; electronic mail: saam@physics.utah.edu

$$P_N(t) = \langle P_A \rangle \frac{\gamma_{se}}{\gamma_{se}+\Gamma}[1 - e^{-(\gamma_{se}+\Gamma)t}], \quad (1)$$

where $\langle P_A \rangle$ is the time- and volume-averaged alkali-metal electron polarization, γ_{se} is the spin-exchange rate, and Γ is the ^{3}He longitudinal relaxation rate, with the corresponding relaxation time $T_1 \equiv 1/\Gamma$. Since typical spin-exchange times are 5–10 h, T_1 must be several tens of hours to obtain noble-gas polarizations approaching $\langle P_A \rangle$, which can normally be kept close to unity.

Contributions to Γ come from bulk He–He binary collisions, gas diffusion through ambient gradients, and from wall collisions. The bulk rate is linear with the ^{3}He density and is usually only significant for cells above several atm; for our room-temperature 8 atm cells it is 0.010 h^{-1}.[11] The Helmholtz coils we use for SEOP (see Sec. VI) provide adequate field homogeneity so that the rate due to diffusion[12,13] for cells of the size and pressure discussed here is negligible. The wall relaxation rate thus practically dictates the quality of a ^{3}He spin-exchange cell, and efforts have been made for more than 30 years to understand and control it. Various glass types, surface treatments, surface coatings, and bakeout procedures have been tried. The results vary widely among research groups and are usually inconsistent and irreproducible. Paradoxically, consistently long polarization lifetimes seem especially difficult to achieve for larger-volume cells, where one would expect a lower surface-to-volume ratio to yield generally slower rates.

Work to understand and control ^{3}He wall relaxation has generally proceeded from the assumption that the major source of such relaxation is paramagnetic impurities on the glass surface. In early work,[14,15] bare borosilicate (Pyrex) and aluminosilicate glass surfaces (such as Corning 1720) were studied. These workers used metastability exchange optical pumping,[8] which does not require an alkali-metal intermediary to produce HP ^{3}He. A local maximum in T_1 (at about 130 K) as a function of temperature in Pyrex[14] suggested the importance of helium permeability, which brings the ^{3}He into close and prolonged contact with the surface. (Quartz is even more permeable than Pyrex,[16] so much so that most quartz cells would leak substantial fractions of their helium to the atmosphere in days or weeks.) Lower permeabilities and overall better results generally led the community toward the use of aluminosilicates,[1,11,17] although these glasses are generally more difficult and expensive to procure, and are more difficult for a glass blower to work than borosilicates. Good results were, however, reported for sealed cells using Corning 7056, a borosilicate glass with much lower helium permeability than Pyrex.[18] An excellent review of the results of many groups using various glasses and coatings for pumping and for storage cells is given in Ref. 19.

We have chosen to continue working with Pyrex, due to its robustness, workability, and easy availability. Moreover, the presence of Rb (which surely coats the cell walls to some degree) chemically alters the surface and inhibits wall relaxation relative to bare Pyrex;[14,19,20] see Sec. VII A. Indeed, in Ref. 14 there was only one cell tested which contained Rb, and that cell had the longest T_1 of all in that work by a large margin. T_1's in the hundreds of hours have been observed in HP ^{3}He storage cells with macroscopic coatings of Rb and Cs metal.[21] These developments, coupled with the discovery of a previously unknown relaxation mechanism involving magnetic surface sites[22] and some trial-and-error testing, have led to our consistent achievement of two benchmarks, $T_1 = 40$ h and $P_N = 40\%$, for large-volume Pyrex ^{3}He spin-exchange cells.

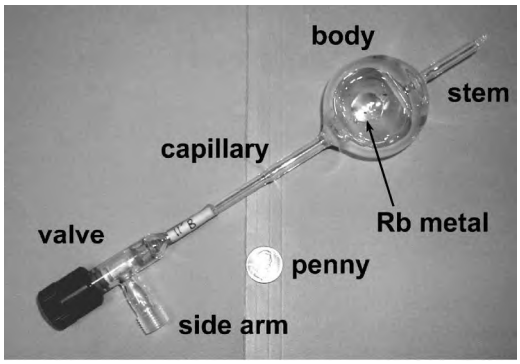

FIG. 1. Pyrex valved spin-exchange cell for generating hyperpolarized ^{3}He. The spherical cell body shown here has a volume of ≈ 50 cm^3. The capillary allows the o-rings in the valve to sit outside the ovens involved both with the initial bakeout (see Sec. IV) and with optical pumping (see Sec. VI).

III. CELL FABRICATION

Our cells are made of standard borosilicate glass (Pyrex), but we have also experimented with quartz and aluminosilicate glasses. The cell body is either spherical ($\approx$4.5 cm i.d.) or cylindrical with rounded ends ($\approx$3 cm i.d. $\times$ 5.5 cm long). The typical total volumes are 50 and 35 cm^3, respectively; see Fig. 1. Recently, we have gone exclusively to spherical cells, as it is easier to produce a surface of uniform thickness, thus minimizing lensing of the incident laser light. The spherical cells generally yield longer T_1's and higher polarizations, although the reasons for this are not clear. We use 32 mm heavy-wall tubing which is "reblown" to the specified inner diameter (i.d.), creating a freshly exposed inner surface. The cells are shaped by blowing the glass on a lathe; cylindrical cells require the additional use of a graphite shaping paddle on the outer surface. A capillary tube, valve, and stem are then attached.

The valve is a right-angle, high-vacuum, all-glass valve.[23] Perpendicular to the valve is attached a threaded glass side arm,[24] through which polarized gas is dispensed and by which the cell is attached to a separate gas-handling system (see Sec. V) for filling with ^{3}He. The valve is attached to the cell via a 10 cm length of glass capillary, which consists of a 6 cm length of 0.5 mm i.d. tubing in series with a 4 cm length of 1 mm i.d. tubing. The wider end is attached to the cell body and helps to prevent the Rb metal from clogging the capillary; the narrow portion is attached to the valve. The gas must pass through the capillary during cell filling and dispensing, so it cannot be impractically narrow. The capillary allows the valve to be kept outside of the oven during optical pumping and suitably lengthens the transit time of a ^{3}He atom from the cell body to the ≈ 1 cm^3 vol-

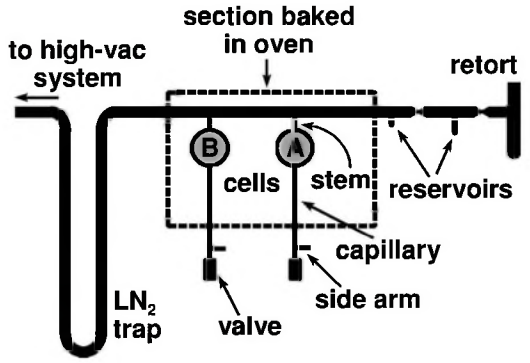

FIG. 2. The glass manifold with two cells attached, as it appears just before being connected to the high-vacuum system (Fig. 3). The top of the retort is flame sealed after a Rb ampule is dropped in. The cells are attached to the manifold at a 55° angle out of the page. Constrictions in the manifold and stems allow for easy pull off. Manifolds are labeled by numbers and cells by letters, starting with the furthest upstream; see Fig. 6.

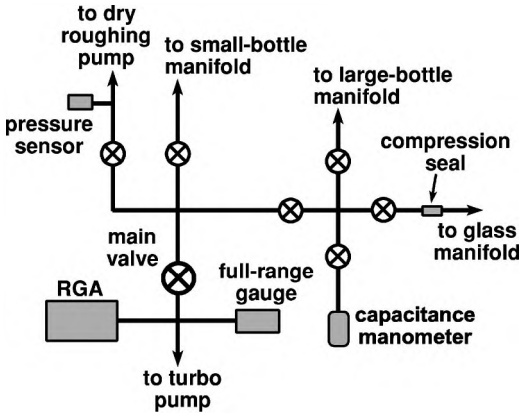

FIG. 3. The oil-free high-vacuum system used for cell fabrication. The glass manifold (Fig. 2) is attached via the compression-seal fitting at right. The construction is stainless steel with packless bellows-sealed valves. Nitrogen purge gas is provided as needed through the connection to the large-bottle manifold.

ume near the valve. Because of the unknown relaxive characteristics of the valve materials and the fact that the valve cannot be baked out well, it is assumed that all ^{3}He atoms that enter the valve volume relax completely. The capillary plays a measurable role in wall relaxation of our long-lifetime cells. By measuring T_1 before and after maneuvering a bead of Rb in the cell to block the capillary, we have estimated its contribution to be $\Gamma_{cap} = 0.002–0.004\ h^{-1}$ at 8 atm pressure; see the Appendix.

A 4 cm length of 6 mm standard-wall tubing (the "stem") is attached opposite to the capillary and connects the cell to a glass manifold for initial evacuation and baking; see Sec. IV. After the cell is flame sealed away from the manifold, the stem accommodates a NMR coil for monitoring the production and decay of HP ^{3}He; see Sec. VI.

The manifold is basically a long tube [primarily 12 mm outer diameter (o.d.) Pyrex] connecting the high vacuum system on one end to an open vertical retort on the other end. The retort accommodates a pre-scored 1 g ampule of 99.93% pure Rb metal.[25] The cells (usually two at a time) are attached orthogonally to the manifold by their stems; see Fig. 2. The manifold includes two small reservoirs used in the Rb distillation process between the retort and the cells. A u-tube liquid nitrogen (LN_2) trap is located between the high-vacuum port and the cells. The LN_2 trap provides additional cryopumping of the manifold, limits backstreaming contamination, and prevents Rb from migrating to the high-vacuum system.

The cells are fabricated and attached to the manifold by our chemistry department's glass blower. The completed manifold is annealed at 560 °C with a soaking time (time for which the glass is held at the maximum temperature) of ≈10 min. The manifold is then allowed to cool slowly for about 45 min. Upon removal from the annealing oven, the open ends are covered with a self-sealing wax film to help prevent ambient moisture or other contaminants from entering and adsorbing to the inner surfaces of the manifold.

IV. CELL PREPARATION

The purpose of careful cell preparation is to remove impurities adsorbed to the surface of the glass and to prevent contaminants from entering. To accomplish this, the cells are baked under vacuum using an oil-free high-vacuum system; see Fig. 3. The construction is stainless steel with copper-gasketed or swaged connecting seals and packless, bellows-sealed valves.[26] The vacuum pump is a turbo-molecular drag pump backed by a diaphragm pump.[27] With the cell manifold attached, the system reaches a base pressure of $\leqslant 4\times10^{-8}$ mbar, monitored at the inlet by a combination cold-cathode/Pirani full-range gauge.[28] Connected opposite the gauge is a residual gas analyzer (RGA),[29] which also functions as a helium leak detector. The gauge and RGA are downstream from the 38 mm stainless steel right-angle main valve. Upstream of this valve are large- and small-bottle gas-handling manifolds, an additional diaphragm roughing pump,[30] and a port for connecting the system to the glass manifold via a 12.7 mm o-ring compression-seal fitting. A 0–1.3 bar capacitance manometer[31] and a solid-state pressure sensor[32] are used for fine and coarse monitoring of upstream pressures. High-purity nitrogen, used as a purge gas, is available through the large-bottle manifold; the attached gas-handling manifolds are generally used for making permanently sealed spin-exchange cells and will not otherwise be described here.

The completed manifold with cells is attached to the vacuum system at the manifold port. This is done while purging the system with research-grade nitrogen gas to help prevent water vapor and oxygen from entering the manifold and vacuum system. The valve stems, with lightly greased ethylene-propylene (alkali-metal resistant) o-rings,[33] are then seated and the cell valves are closed. An ampule of Rb is opened in the flow of N_2 from the retort and is dropped, open end down, into the retort. The purge gas is turned off, and the retort is flame sealed shut. With the manifold now sealed from the external environment, it is evacuated with the roughing pump, opened to the turbo pump, and tested for leaks with the RGA. Minor leaks can often be repaired on the spot, while more serious problems may have to be sent back to the glass blower. Finally, with the manifold sealed and leak tight, LN_2 is added to the Dewar surrounding the trap.

The manifold is then baked continuously at about 400 °C for 2–4 days. We now use a home-built, insulated, steel-walled oven designed especially for these manifolds. We previously wrapped the manifold in heating tape and aluminum foil. The oven heats stably and uniformly (within a few degrees), avoiding hot spots that can develop from the use of heating tape; it also greatly reduces setup time and the risk of damaging the delicate manifold due to overhandling. The cells are attached to the manifold at a 55° angle from vertical (see Fig. 2) to allow the valves to protrude laterally through a cut out in the oven (to avoid damaging the o-rings). The oven is blanketed by 25-mm-thick ceramic fiber insulation,[34] which is covered with high-temperature silica cloth.[35] This blanket keeps the valves near room temperature, even though they are only a few centimeters from the oven. Heat is provided by a 1.8 kW, 120 Vac ceramic strip heater[36] located on the oven floor, which is controlled by a 2 kW, 120 Vac solid-state dimmer switch. A 50 Vac input is sufficient to maintain the baking temperature. The retort and distillation reservoirs also protrude out of the oven; these are wrapped in heating tape and aluminum foil, which can be removed as necessary as Rb distillation progresses. Temperatures are monitored with type-E thermocouples placed both in the oven and on the manifold under the heater tape and foil.

After about 24 h of baking, the Rb metal is liquified for the first time by brief exposure to a flame, which allows any trapped gases to escape and be pumped away. After allowing the retort to cool, Rb is distilled from the retort to the first reservoir. First, the foil and heat tape are unwrapped from the retort to 3 cm beyond the first distillation reservoir, and this section is allowed to cool. The Rb is then "chased," i.e., heated and evaporated with a cool methane–oxygen flame (not so cool that carbon deposits, which inhibit visibility, are left on the glass), driving it into but not beyond the first reservoir. The idea here is to volatilize all of the Rb that is eventually to be chased into the reservoir, leaving less volatile contaminants in the retort. The flame is not held in one spot on the glass long enough to produce any orange sodium glare; this avoids softening of the glass or its reaction with Rb. Effective chasing requires 30–45 min and benefits from some practice. When completed, contaminants (e.g., Rb oxides and RbOH) and about 10%–20% of the Rb metal are left behind in the retort, which is then flame sealed away from the manifold.

After 12–24 h of further baking, Rb is chased to the second reservoir by a similar procedure. The cells are allowed to bake for yet another 12–24 h before the oven is turned off and allowed to cool completely. Rb is then chased into the cells, starting with the one closest to the retort (cell "A"). The capillary is kept hot during this step so that it will not become clogged with Rb. After 100–300 mg of Rb is distilled in, the cell is flame sealed from the manifold. The process is repeated for the remaining cell(s), working downstream.

We have found a difference in convenience only, and not in cell quality, with the introduction of the baking oven. We also find no difference in the case where the Rb is distilled into all of the cells in one step before they are each sealed from the manifold. We note that the amount of Rb distilled in does matter; amounts significantly less than about 100 mg generally result in cells with poor wall characteristics. The relationship between Rb and wall relaxation is discussed further in Sec. VII A. The baking time and temperature have not been optimized experimentally, but these seem reasonable based on the ideas that (1) we wish to bake as hot as possible without approaching the annealing point of the glass and (2) the base vacuum pressure and RGA spectrum change very little after a day or so of baking. Our ability to consistently produce quality cells has compelled us not to experiment much with our bakeout parameters or other aspects of the fabrication protocol.

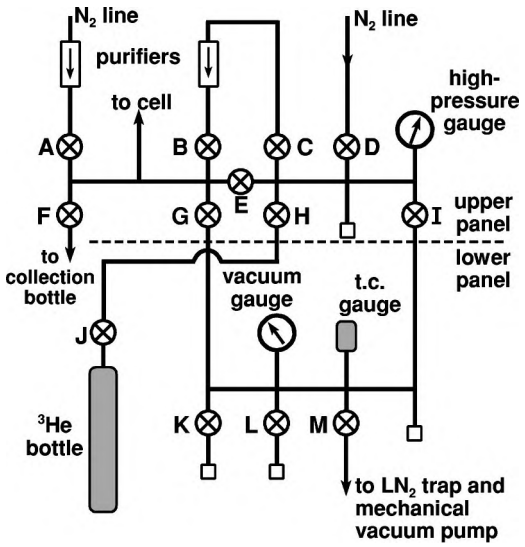

FIG. 4. Gas-handling system used to fill cells with ^{3}He. This system is completely separate from the high-vacuum system (Fig. 3) used for bakeout and Rb distillation. Cells can be refilled indefinitely with no change in the ^{3}He wall-relaxation time. The valves and bottle are all mounted to two vertical plates on a relay rack. The dashed line marks the boundary between the upper and lower plates. Open squares represent auxiliary ports. The collection bottle is used to save ^{3}He that would otherwise be discarded after cell filling.

V. CELL FILLING SYSTEM

A separate, home-built vacuum and gas-handling system is used to fill and refill cells; see Fig. 4. This system is similar to one built previously by Saam and Conradi.[5] It is constructed of 6.4 mm o.d., 4.8 mm i.d. stainless steel tubing with weld and swage fittings. The packed, nonrotating-stem valves[37] are labeled by letters, as shown in Fig. 4. The system, built vertically on two large aluminum plates affixed to a relay rack, is divided into an upper gas-handling and purification manifold and a lower vacuum manifold; these are connected at two points by valves (I) and (G). The vacuum manifold has a dial gauge and a thermocouple gauge to monitor pressure. Below valve (M) is a u-tube LN_2 trap followed by a 150 L/min rotating-vane mechanical pump. The pump has a Micromaze[38] trap at the inlet to further inhibit oil backstreaming.

The upper manifold is essentially a fill path from the gas bottle to the cell. When new, the lecture bottle contains 25 atm·L of research-grade ^{3}He (99.99% pure) mixed with 2% nitrogen, at a total pressure of 55.4 bar. The 3 cm^3 volume

bounded by the bottle valve and valve (J) is the charging volume used for a new bottle. As the gas is used up and the bottle pressure decreases, the 12 cm^3 charging volume up to valve (H) is employed. The gas is conducted through a purifier[39] bounded by valves (B) and (C), and then to the cell through a 1 m length of 1.6 mm i.d. stainless steel (ss) capillary tubing. The flexible ss capillary provides stress relief for the cell and a low dead volume for filling. The cell is placed in a secure wooden box (mounted to the side of the relay rack) with its glass capillary and valve protruding. It is attached, using the compression-seal fitting on the side arm, to the ss capillary tube via a custom-built tee connector. The other outlet of the tee is exhausted to room air through a flow meter and one-way pressure-relief valve. Because of the low conductance of the ss capillary, a N_2 purge line with purifier is provided and used in addition to evacuation to keep the system clean. The two identical gas purifiers discussed here are designed for use with nitrogen but are also adequate for use with noble gases.

Initially, the cell (with its valve closed) is attached to the tee connector with the compression seal loose. A N_2 purge is passed through the capillary at 0.2 l/min for 20 min. After the purge, the compression seal is tightened, valve (A) is closed, and the fill line is evacuated through valve (G). The system remains under vacuum for tens of minutes to hours. A series of at least three backfill/evacuate sequences [closing valve (G), filling the ss capillary and cell side arm with purge gas, then re-evacuating] is completed to help remove room air that may have entered when the cell was attached.

When the evacuation procedure is complete, valve (G) is closed, and the cell valve is opened in preparation for filling. The cells are filled in a series of charges. At the start of each charge, all valves except the cell valve are closed. The bottle is opened to the charging volume and closed again immediately. The valves (H), (C), and (B) are successively opened until the pressure measured by the 0–200 psig dial gauge equilibrates. Valves are opened gradually, so that the gas can be metered; this is particularly important in opening valves (C) and (B), since the purifier is effective only at flow rates below 0.2 l/min. In our system, staying below this rate is assured by watching the pressure gauge and keeping the rate of change in pressure below about 2 psi/s. At equilibrium, all valves except the cell valve are closed again. This procedure is repeated until the desired cell pressure is reached; we typically fill cells to 8 atm (absolute pressure). When the desired final pressure is reached, the cell valve is closed, and all other valves in the filling path are closed to preserve the gas contained therein for future use. The filling path from the bottle to valve (B) is evacuated and pumped on only occasionally, such as when the ^{3}He bottle is replaced. The remaining ^{3}He is collected into a large ballast volume (an otherwise empty gas cylinder) for recycling.

VI. THE POLARIZER

The polarizer consists mostly of an aluminum-frame cart (approx. 2 m long, 0.6 m deep, and 1 m high) with a top surface for mounting optical components and shelving below. The cart has a built-in 45 cm diam. Helmholtz pair (200 turns of 14 American Wire Gauge wire per coil), which produces a 30 G field when driven in parallel with 12 V at 8 A.

A welded aluminum box covered with fiberboard insulation serves as an oven. It is located at the center of the Helmholtz pair and is heated by air forced through a filament-heater pipe[40] attached to the cart. The temperature is maintained to a few tenths of a degree with a resistive temperature detector and controller.[41] A cradle at the center of the oven holds the cell body; the capillary protrudes out one side of the oven to avoid heating the valve. The top plate and the top half of the side plate above the capillary are welded together and can be removed as a unit for internal access. Round windows (5 cm diameter) are located on four sides—for laser entry, laser exit, on top, and laterally opposite the capillary. The latter two are for monitoring fluorescence from the cell during SEOP. Window glass (6.4 mm thick) is used throughout, double paned for extra insulation except at the laser-entrance window. (Laser transmittance through this window could be improved by a few percent by using an optical flat, antireflection coated for 795 nm.) The oven temperature is typically set for 160° C, although based on the characteristic time we observe to polarize cells (Fig. 5), the actual cell temperature is 170–180 °C, where the saturated vapor density of Rb is about $2.5–4.5\times 10^{14}$ cm^{-3};[42] see Sec. VII B. The temperature difference is caused by the large laser power: the N_2 gas in the cell heats up due to increased collisional deexcitation of Rb atoms.[43]

The laser and optics train are mounted on an optical rail to one side of the coils and oven. The laser is a 795 nm, 40 W diode array[44] with a full width at half maximum linewidth of about 1.7 nm. The laser is resonant with the 795 nm D_1 transition in Rb. It is mounted to an aluminum block which is water cooled by a closed-loop refrigerator[45] with built-in temperature control to a few tenths of a degree. Cylindrical optics are used to collimate the fast and slow axes separately. A 76 mm diam. mica quarter-wave plate[46] circularly polarizes the light just before it enters the oven. Rubidium-vapor absorption is monitored by a PC plug-in miniature spectrometer[47] with 0.3 nm resolution coupled by a fiber optic to the light emerging from the laser exit window. When the laser is at the proper frequency, the computer displays the laser line with a central dip corresponding to absorption by the vapor. Laser fluorescence is visually monitored with surveillance-system cameras and a small TV monitor. The cameras are sensitive in the near infrared and are equipped with interference filters[48] for the Rb D_2 resonance (780 nm). The D_1 and D_2 states are mixed after a Rb atom absorbs a photon;[9] monitoring D_2 fluorescence thus effectively separates fluorescence from laser scatter. The beam profile can then be matched to the cell dimensions by adjusting lens positions.

The ^{3}He polarization is monitored by a home-built 100 kHz pulse NMR spectrometer;[49] the multi-turn coil (inductance $L\approx 800$ μH, quality factor $Q\approx 50$) is placed around the stem of the cell inside the oven. The aluminum walls of the oven are grounded and provide adequate rf shielding. Figure 5 shows samples of a free-induction decay (FID), polarization transient ("spin up"), and room-temperature decay transient ("spin down") for ^{3}He in a typical 8 atm cell.

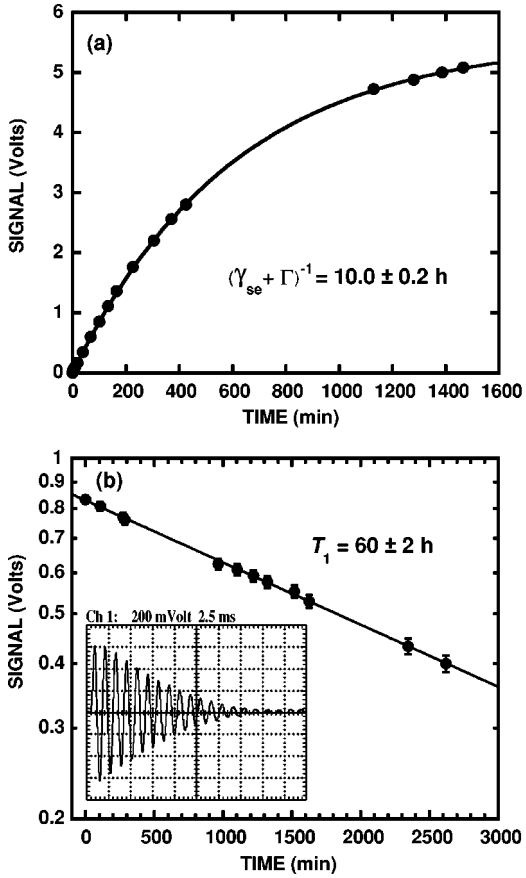

FIG. 5. (a) Typical ^{3}He polarization transient for cell 8A at 8 atm in a 30 G magnetic field. The curve is a best fit to Eq. (1), yielding the characteristic spin-up time of 10 h. Although the oven temperature was set to 160 °C, the spin-up time corresponds to 170–180 °C. The temperature increase is due to the laser heating of the cell. (b) Subsequent room-temperature decay transient at 30 G for the same cell, measuring the combined wall and bulk relaxation rates. The line is a best fit to a single exponential decay. One deduces a wall-relaxation time for this cell of ≈150 h, since the bulk time is ≈100 h. Inset: A typical ^{3}He FID acquired at 30 G (100 kHz); the initial FID amplitude provides the data for spin-up and spin-down measurements.

VII. EXPERIMENTAL RESULTS

A. T_1 measurements

All measurements of the longitudinal relaxation time T_1 for our cells were made at room temperature and at 30 G, unless otherwise indicated. These are relevant conditions for HP-gas production, since high fields are not necessary to generate the polarization, and a 30 G Helmholtz pair is inexpensive and portable. Very low flip angles (<5°) were used to generate a FID at appropriate time intervals with negligible loss of polarization. The initial height S of the FID was recorded as a function of time and fit to $S(t) = S(0)\exp(-t/T_1)$ to extract T_1. (The thermal equilibrium signal is negligible for our conditions.)

We have recently discovered that T_1 at 30 G is dramatically reduced (factors of 2–20) solely by intervening exposure of a cell to a large magnetic field (of order 0.1 T or greater). The original T_1 can be restored by demagnetizing or degaussing the cell, i.e., rotating it at about 1 Hz in a field which is gradually reduced to zero from about 1 T. (Magnetization and degaussing were conveniently done in a 1 T iron-core electromagnet.) The effect, termed "T_1 hysteresis," is due to multi-domain magnetic sites at or near the glass surface. These sites become magnetized in a large field and have a significant remanent magnetization when the cell is returned to 30 G, leading to a stronger interaction with colliding ^{3}He spins and a shorter T_1. The effect has been observed in borosilicate, aluminosilicate, and quartz glasses and is correlated with the presence of the Rb necessary for SEOP. Indeed, the effect should be observable to some degree in almost all spin-exchange cells. The details of T_1 hysteresis are discussed in Ref. 22.

We have consistently produced cells with T_1's in excess of 40 h. The measured T_1's are generally robust and reproducible (to 10% or so), although the cell is refilled several times and/or repeatedly exposed to the 40 W laser at temperatures of 160–200 °C. The results of T_1 measurements on many of our cells are shown in Fig. 6. The wall relaxation

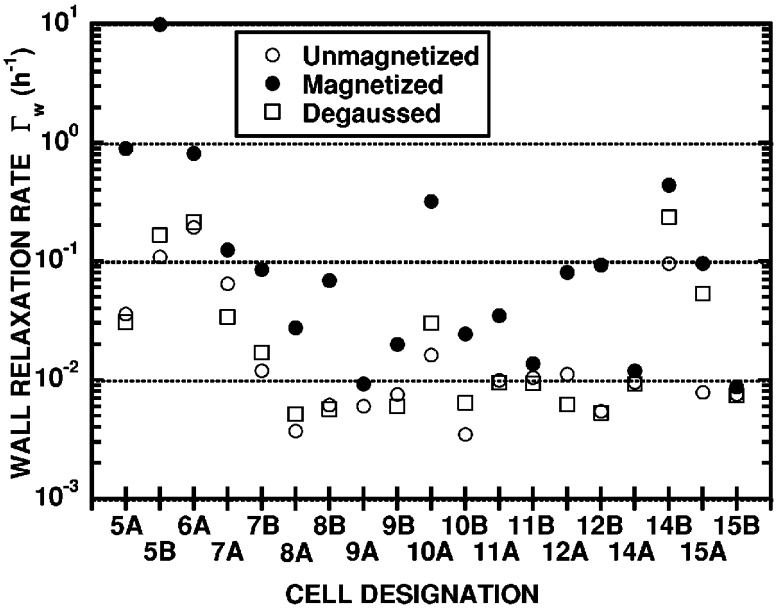

FIG. 6. The wall relaxation rate Γ_w at 30 G plotted vs cell designation for 19 of approximately 30 ^{3}He spin-exchange cells fabricated in our laboratory. These cells all contain Rb, except for 12A and 12B, which contain potassium. The manifolds are numbered chronologically; "A" and "B" refer to a pair of cells made on the same manifold (Fig. 2). The bulk ^{3}He–^{3}He relaxation rate of 0.010 h^{-1} for 8 atm has been subtracted for each cell. Prior to being magnetized at 1 T or after degaussing, most cells have $\Gamma_w \approx 0.01$ h^{-1} or smaller, meaning a measured $T_1 \geqslant 50$ h.

rate Γ_w is shown for each cell before exposure to a high field (unmagnetized), magnetized, and degaussed. The bulk contribution (0.010 h^{-1} at 8 atm[11]) has been subtracted from the data. T_1 hysteresis occurs to some degree for all cells over a broad range of initial unmagnetized lifetimes (a few hundred minutes to tens of hours), indicating that the variation in rates from cell to cell may be due to differences in the size and/or concentration of magnetic sites. In any case, it is necessary to avoid exposure of most cells to large magnetic fields (the onset of T_1 hysteresis occurs at a few hundred gauss[22]) or to degauss them before they are used for SEOP.

In addition to its crucial role in optical pumping, the presence of alkali metal in SEOP cells inhibits wall relaxation while simultaneously giving rise to T_1 hysteresis.[22] Almost all of the cells represented in Fig. 6 contain Rb (cells 12A and 12B contain potassium). We also made several otherwise identical cells containing no alkali metal. Prepolarized ^{3}He was then introduced in order to measure T_1 on bare Pyrex. For these cells T_1 was typically less than 10 h, and no hysteresis was observed. The Rb may be chemically neutralizing paramagnetic sites or inhibiting permeation of ^{3}He into the glass; see Sec. II and Refs. 14 and 15. At the same time, the Rb introduces T_1 hysteresis, presumably by creating magnetic sites. Our current working hypothesis is that the Rb acts as a reducing agent, converting iron ions and oxides to multi-domain metallic iron.

B. Polarimetry

Using our benchmark T_1 of 40 h, the measured Rb–^{3}He spin-exchange rate at 180 °C,[50,51] the saturated vapor pressure curve for Rb,[42] and Eq. (1), the theoretical limit of attainable ^{3}He polarization is about 80%, given $\langle P_{\mathrm{Rb}}\rangle = 100\%$. We estimate (and other research groups have shown directly[52]) that $\langle P_{\mathrm{Rb}}\rangle$ can be maintained at nearly 100% under these conditions with a diode-laser array such as the one we use; yet there are no reports in the literature of ^{3}He polarizations above about 50%. This polarization deficit remains unexplained at present.

We measure the absolute polarization of HP ^{3}He by comparing the NMR signal from the ^{3}He cell to a proton signal provided by a water sample in thermal equilibrium. The water sample has a geometry similar to the ^{3}He cell and contains a sufficient amount of dissolved $CuSO_4$ to reduce the proton T_1 to less than 100 ms. The comparison is done at a common NMR frequency, high enough for sufficient proton signal. Since the proton polarization can be calculated, and the spin densities of both samples are known, the ^{3}He polarization can be determined by measuring the ratio of NMR signals from the two samples. (The polarization is independent of applied field for hyperpolarized gases.) In the low-flip-angle limit, the signal ratio S_3/S_1 is given by[49]

$$\frac{S_3}{S_1}=\frac{P_3}{P_1}\frac{n_3}{n_1}\frac{\gamma_3^2}{\gamma_1^2}, \tag{2}$$

where P is polarization, γ is gyromagnetic ratio, n is spin density, and the subscripts "3" and "1" refer to ^{3}He and protons, respectively. The spin density for the ^{3}He cell can be calculated from the pressure measured when it is filled. When solved for P_3 using water, Eq. (2) can be expressed

$$P_3=(3.76\times 10^{-4})\frac{f}{p}\frac{S_3}{S_1}, \tag{3}$$

where f is the common NMR frequency in megahertz, and p is the cell pressure in atmospheres at room temperature. For our cells, S_3/S_1 is typically 40–50 dB. Figure 7 shows a pair of FIDs at 32.5 MHz on the same oscilloscope voltage scale. The ^{3}He FID is a single acquisition from an 8 atm cell with 50 dB attenuation in the signal line; the proton FID is four averaged signals with no signal-line attenuation. Using Eq. (3) and factoring in the slight difference in the two FID amplitudes, the ^{3}He polarization is $P_3=50\pm 4\%$. The uncertainty comes from the measurement of the proton FID height and from small losses in transporting the cell from the polarizer to the electromagnet.

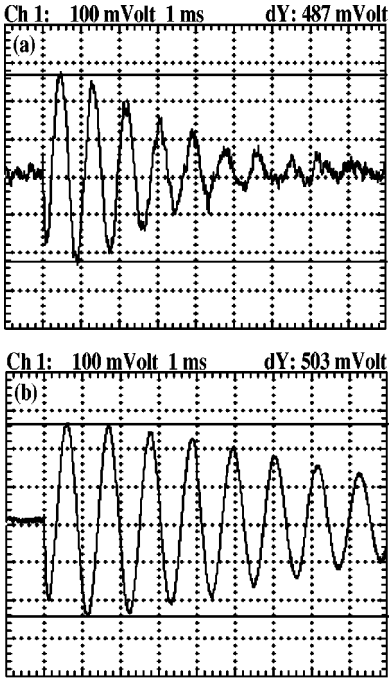

FIG. 7. Two FIDs acquired at 32.5 MHz using the exact same NMR equipment and settings; only the field is different. The flip angle is $<10°$ in both cases. The peak-to-peak voltage of the first full oscillation is marked by the solid horizontal cursor lines. (a) Four averaged water proton signals acquired at 0.763 T. (b) A single acquisition at 1.00 T from an 8 atm ^{3}He cell with 50 dB of signal-line attenuation relative to (a). Using Eq. (3), the (field-independent) ^{3}He polarization is $50\pm 4\%$. The transverse coherence time is dominated by field gradients and is longer in (b) because of the better field homogeneity in the electromagnet at higher fields.

C. Overall performance

We now routinely fabricate SEOP cells that reach a "40/40" benchmark: ^{3}He polarization $\geqslant 40\%$ and a relaxation lifetime $T_1 \geqslant 40$ h. The maximum polarization is achieved in 12–20 h in about 0.5 atm·L of gas, although polarizations as high as 20% are achieved in 3–5 h. The system can be left to run overnight unattended in order to achieve maximum po-

larization. The apparatus described here cost $35–40k to build; about $15k of that total was spent on the high-vacuum system.

A few other research groups and at least one company, Amersham Health (AH), have put some effort into high-volume, high-throughput devices to generate HP ^{3}He. With the exception of Gentile, *et al.*,[19] there are few details of these systems described in the open literature. Recent papers from the University of Virginia group describe the AH system (which also uses SEOP but is not yet commercially available) as capable of up to 35% polarization in ≈ 1 atm·L of gas after several hours.[6,53] Our system is roughly comparable, although our spin-exchange rates are typically somewhat lower. We note that while we have yet to use our system for human studies, the group at Washington University has obtained the necessary FDA exemption for a system very similar to ours.

Groups at the National Institute of Standards and Technology (NIST) in Gaithersburg, MD and at Mainz University in Germany have employed the technique of metastability exchange optical pumping (MEOP).[8] The Mainz group can produce ≈ 1 atm·L of 55% polarized ^{3}He in about 2 h.[54] As with all MEOP systems, the gas must be compressed from a few Torr up to atmospheric pressure with minimal polarization loss. A two-stage titanium piston compressor is employed for this purpose. The disadvantages of this system are its size, complexity, and nonportability. Our system is portable enough to have been recently driven from Salt Lake City to Richland, WA, for collaborative MRI experiments at Pacific Northwest National Laboratory. At NIST, a compact and portable device for gas compression involving a modified diaphragm pump has been developed. For MRI applications, it is expected to produce ≈ 1 atm·L of 20% polarized gas in about 2 h.[19] We achieve substantially higher final polarization than the NIST system at the expense of considerable pumping time.

VIII. CONCLUSION

We have developed a successful protocol for fabrication of large-volume, valved ^{3}He spin-exchange cells for MRI from inexpensive and easily worked Pyrex glass. We have identified an important mechanism for wall relaxation that has been directly confirmed experimentally by studies of T_1 hysteresis, and we have confirmed the importance of Rb metal (in amounts of order 100 mg or more) for long wall-relaxation times.

We have yet to reach the ultimate goal of understanding the physics of the cell fabrication process at each step, but we have detailed here some progress away from cell-making "voodoo." The filling of cells has been separated from the rest of the process and is done on a separate gas-handling system. Cell properties are determined and, so far as we know, fixed by one or more of the earlier steps (glass blowing, evacuation, baking, and Rb distillation). Once sealed from the high-vacuum system, cells can be refilled indefinitely with no significant change in their wall properties. Based on the comparative previous experience of one of us (B. T. S.) with several cell-fabrication systems, we can make an educated guess that the important elements of cell preparation include the clean, oil-free turbo-molecular pump, the u-tube LN_2 trap included on the glass manifold, and the multi-stage distillation of the Rb metal into the cells. Our vacuum system does not qualify as UHV and is not entirely metal sealed, although the stainless-steel construction and good vacuum practice (e.g., keeping air and water out of the system at all possible times) presumably help to further minimize contaminants in the manifold.

The discovery of T_1 hysteresis has opened the door to learning more about cell fabrication by finally providing a concrete lead as to the mechanism involved in glass-surface relaxation of ^{3}He. The detection of magnetism in Rb-coated glass with a second method [electron spin resonance (ESR) or vibrating-sample magnetometry, for example] would confirm the effect and, in conjunction with further NMR measurements, potentially allow better determination of the chemical identity, size, concentration, and magnetic moment of the magnetic sites. It may eventually prove possible to eliminate the sites altogether, perhaps improving T_1 still further and making cells even more robust in high-field environments, such as in or near a MRI magnet.

More detailed schematics and plans of any of the apparatus described here can be obtained by contacting the authors.

ACKNOWLEDGMENTS

The authors gratefully acknowledge many useful discussions with M. S. Conradi and J. C. Leawoods at Washington University, as well as the expert glass blowing of J. Kyle. This work was supported by a grant from the Whitaker Foundation.

APPENDIX: TRANSIT TIME OF ^{3}He IN THE CAPILLARY

As discussed in Sec. III, the valve on our refillable ^{3}He spin-exchange cells is separated from the cell body by a glass capillary tube (see Fig. 1), so that the potentially relaxive components of the valve are isolated from the bulk gas. Here we calculate Γ_{cap}, the ^{3}He relaxation rate due to the capillary and valve. The analysis here is based in part on notes from discussions with both H. L. Middleton and M. S. Conradi. We assume a capillary of length L, radius r, and cross section $A=\pi r^2$. We assume that the diffusion time, both across the cell and between the cell and the valve, is short compared to the polarization lifetime T_1, that T_1 is dominated by wall relaxation, and that the cell has a uniform relaxivity η, so that the wall-relaxation rate Γ_w is given everywhere by

$$\Gamma_w=\eta\frac{S}{V}, \tag{A1}$$

where S/V is the surface to volume ratio, equal to $2/r$ for the cylindrical capillary. We consider the case in which the magnetization M_0 in the cell body may be considered constant. We note that it is quite possible that η in the capillary is larger than in the body (due, for example, to the low conductance during the bakeout or to the capillary coming from a

different batch of Pyrex). We deal with this possible difference below. In the capillary, the diffusion equation for ^{3}He magnetization $M(x)$ in one dimension is

$$\frac{\partial M(x)}{\partial t} = D\frac{\partial^2 M(x)}{\partial x^2} + Q(x), \tag{A2}$$

where D is the diffusion coefficient of ^{3}He atoms in the cell and $Q(x)$ is a source term. Under steady-state conditions with $Q(x) = -\Gamma_w M(x)$ and using Eq. (A1) we obtain

$$\frac{d^2}{dx^2}M(x) = \frac{\eta S}{DV}M(x) = \frac{2\eta}{Dr}. \tag{A3}$$

The general solution to Eq. (A3) is

$$M(x) = C\sinh(qx) + K\cosh(qx), \tag{A4}$$

where

$$q^2 = 2\eta/Dr. \tag{A5}$$

We assume that the valve at $x=0$ instantly relaxes all spins with which it comes in contact. The boundary conditions are thus $M(0)=0$ and $M(L)=M_0$. Hence, we must have $K=0$, and the particular solution is

$$M(x) = \frac{M_0}{\sinh(qL)}\sinh qx. \tag{A6}$$

The flux of magnetic moment $J(x)$ through a plane of constant x in the capillary is thus

$$J(x) = -D\frac{dM(x)}{dx} = -\frac{DM_0 q}{\sinh(qL)}\cosh(qx) \tag{A7}$$

and the total magnetic moment per unit time flowing into the cell at the capillary opening is

$$AJ(L) = -\pi r^2 DM_0 q\coth(qL). \tag{A8}$$

Hence, the effective relaxation rate due to the capillary and valve is

$$\Gamma_{\text{cap}} = -\frac{AJ(L)}{M_0 V_c} = \frac{\pi r^2 Dq\coth(qL)}{V_c}, \tag{A9}$$

where V_c is the cell volume. In our case, η is usually small, and in the limit $qL \ll 1$

$$\Gamma_{\text{cap}} = \frac{\pi r^2 D}{V_c L}. \tag{A10}$$

Note that in this limit, Γ_{cap} is independent of η, and a modest increase in η in the capillary compared to the cell body would be irrelevant.

Based on $T_1 = 40$ h for a spherical cell 4.5 cm in diameter, we estimate $\eta \approx 5\times10^{-6}$ cm/s. For an 8 atm cell, $D = 0.23$ cm^2/s for ^{3}He at 295 K.[55] Using $r = 0.025$ cm and $L = 6$ cm for the narrow portion of the capillary and Eq. (A5), we obtain $qL = 0.25$. Using Eq. (A10), we calculate $\Gamma_{\text{cap}} \approx 0.008\ \text{h}^{-1}$. This number is a factor of 2–4 greater than the measured range for Γ_{cap} given in Sec. III for our cells. The discrepancy has at least two potential sources: the additional 4 cm of 1 mm i.d. capillary in our cells was not included in this calculation, and the valve may not be perfectly relaxing [i.e., we may have $M(0)>0$].

[1] G. L. Jones, T. R. Gentile, A. K. Thompson, Z. Chowdhuri, M. S. Dewey, W. M. Snow, and F. E. Wietfeldt, Nucl. Instrum. Methods Phys. Res. A **440**, 772 (2000).
[2] M. V. Romalis and M. P. Ledbetter, Phys. Rev. Lett. **87**, 067601 (2001).
[3] H. J. Jänsch, T. Hof, U. Ruth, J. Schmidt, D. Stahl, and D. Fick, Chem. Phys. Lett. **296**, 146 (1998).
[4] T. Pietraβ, R. Seydoux, and A. Pines, J. Magn. Reson. **133**, 299 (1998).
[5] J. C. Leawoods, D. A. Yablonskiy, B. Saam, D. S. Gierada, and Mark S. Conradi, Concepts Magn. Reson. **13**, 277 (2001).
[6] E. E. de Lange, J. P. Mugler III, J. R. Brookeman, J. Knight-Scott, J. D. Truwit, C. D. Teates, T. M. Daniel, P. L. Bogorad, and G. D. Cates, Radiology **210**, 851 (1999).
[7] T. G. Walker and W. Happer, Rev. Mod. Phys. **69**, 629 (1997).
[8] F. D. Colegrove, L. D. Schearer, and G. K. Walters, Phys. Rev. **132**, 2561 (1963).
[9] W. Happer, Rev. Mod. Phys. **44**, 169 (1972).
[10] M. V. Romalis, E. Miron, and G. D. Cates, Phys. Rev. A **56**, 4569 (1997).
[11] N. R. Newbury, A. S. Barton, G. D. Cates, W. Happer, and H. Middleton, Phys. Rev. A **48**, 4411 (1993).
[12] L. D. Schearer and G. K. Walters, Phys. Rev. **139**, A1398 (1965).
[13] G. D. Cates, S. R. Shaefer, and W. Happer, Phys. Rev. A **37**, 2877 (1988).
[14] W. A. Fitzsimmons, L. L. Tankersley, and G. K. Walters, Phys. Rev. **179**, 156 (1969).
[15] R. S. Timsit, J. M. Daniels, and A. D. May, Can. J. Phys. **49**, 560 (1971).
[16] F. J. Norton, J. Appl. Phys. **28**, 34 (1957).
[17] J. R. Johnson, A. K. Thompson, T. E. Chupp, T. B. Smith, G. D. Cates, B. Driehuys, H. Middleton, N. R. Newbury, E. W. Hughes, and W. Meyer, Nucl. Instrum. Methods Phys. Res. A **148**, 356 (1995).
[18] T. B. Smith, T. E. Chupp, K. P. Coulter, and R. C. Welsh, Nucl. Instrum. Methods Phys. Res. A **402**, 247 (1998).
[19] T. R. Gentile, D. R. Rich, A. K. Thomptson, W. M. Snow, and G. L. Jones, J. Res. Natl. Inst. Stand. Technol. **106**, 709 (2001).
[20] M. F. Hsu, G. D. Cates, I. Kominis, I. A. Aksay, and D. M. Dabbs, Appl. Phys. Lett. **77**, 2069 (2000).
[21] W. Heil, H. Humblot, E. Otten, M. Schafer, R. Surkau, and M. Leduc, Phys. Lett. A **201**, 337 (1995).
[22] R. E. Jacob, S. W. Morgan, B. Saam, and J. C. Leawoods, Phys. Rev. Lett. **87**, 143004 (2001).
[23] Part No. 826460-004, Kimble/Kontes, Vineland, NJ.
[24] Part No. CG-351-01,Chemglass Inc., Vineland, NJ.
[25] Atlantic Metals and Alloys, Stratford, CT.
[26] Part No. SS-8BK-K5, Nupro Co., Willoughby, OH.
[27] Model No. TSU071E, Pfeiffer Vacuum Inc., Nashua, NH.
[28] Model No. PKR-251, Pfeiffer Vacuum Inc., Nashua, NH.
[29] Model No RGA200, Stanford Research Systems, Sunnyvale, CA.
[30] Model No. MVP015-T, Pfeiffer Vacuum Inc., Nashua, NH.
[31] Part No. VCMT-1000-BA, Varian Vacuum, Lexington, MA.
[32] Part No. NPC-410, Lucas Novasensor, Fremont, CA.
[33] Part Nos. CG-303-108 and CG-303-101, Chemglass Inc., Vineland, NJ.
[34] Part No. 370-5, Cotronics, Inc., Brooklyn, NY.
[35] Part No. 18S-36, Thermostatic Industries, Los Angeles, CA.
[36] Omega Heater, Inc., Ronkonkoma, NY.
[37] Part No. SS-14DKS4, Whitey Co., Highland Heights, OH.
[38] Part No. MMA-077-2QF, Kurt J. Lesker Co., Clairton, PA.
[39] Part No. 00040-VCR-N2, Nupure Inc., Manotick, Ontario, Canada.
[40] Part No. AH75-6MF, Hotwatt Inc., Danvers, MA.
[41] Part Nos. CN76000 and F3105, Omega Engineering Inc., Stamford, CT.
[42] T. Killian, Phys. Rev. **27**, 578 (1926).
[43] D. K. Walter, W. M. Griffith, and W. Happer, Phys. Rev. Lett. **86**, 3264 (2001).
[44] Model B1-79-40C-19-30-A, Coherent Semiconductor, Santa Clara, CA.
[45] Model Affinity RAA-003A-CB01CB, Lydall Inc., Ossipee, NH.
[46] Model WMPS-795-30-4, CVI Laser Inc., Albuquerque, NM.
[47] Model PC2000, Ocean Optics, Inc., Dunedin, FL.
[48] Part No. XA46-780NB2, Omega Optical Inc., Brattleboro, VT.

[49] B. Saam and M. S. Conradi, J. Magn. Reson. **134**, 67 (1998).
[50] A. B. Baranga, S. Appelt, M. V. Romalis, C. J. Erickson, A. R. Young, G. D. Cates, and W. Happer, Phys. Rev. Lett. **80**, 2801 (1998).
[51] B. Larson, O. Häusser, P. P. J. Delheij, D. M. Whittal, and D. Thiessen, Phys. Rev. A **44**, 3108 (1991).
[52] T. G. Walker (private communication).
[53] T. A. Altes, P. L. Powers, J. Knight-Scott, G. Rakes, T. A. E. Platts-Mills, E. E. de Lange, B. A. Alford, J. P. Mugler III, and J. R. Brookeman, J. Magn. Reson Imaging **13**, 378 (2001).
[54] W. Heil, J. Dreyer, D. Hofmann, H. Humblot, E. Lelievre-Berna, and F. Tasset, Physica B **267,268**, 328 (1999).
[55] R. Barbé, M. Leduc, and F. Laloë, J. Phys. (Paris) **35**, 935 (1974).